ACS OMEGA

Open Access

http://pubs.acs.org/journal/acsodf

Article

Novel DNA Biosensing Platform for Detecting HIV Integrase for Highly Sensitive and Quantitative HIV Detection, Diagnosis, and Therapeutic Monitoring

Fuming Chen, Jing Wang, Jie Ma, Li Song, Haojie Yan, Feng Wang,* Zhengrong Yang,* and Furong Li*

Cite This: *ACS Omega* 2024, 9, 25042−25053

Read Online

ACCESS | Metrics & More | Article Recommendations | Supporting Information

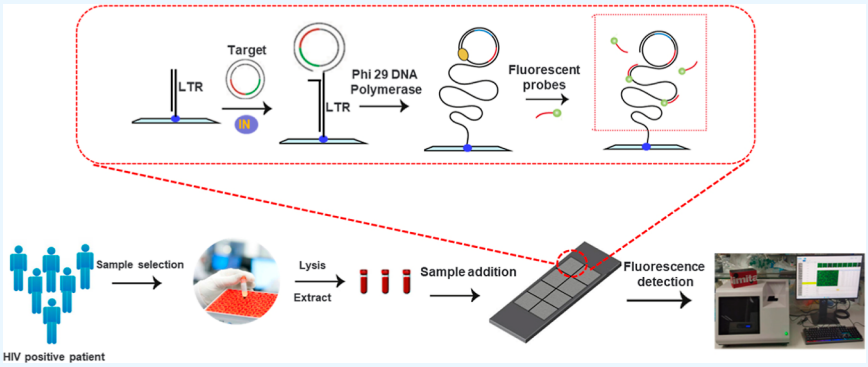

ABSTRACT: Straightforward, sensitive, and specific human immunodeficiency virus (HIV) assays are urgently needed. The creation of a point-of-care (POC) device for decentralized diagnostics has the potential to significantly reduce the time to treatment, especially for infectious diseases. Notably, however, many POC solutions proposed to date fall short of meeting the ASSURED guidelines, which are crucial for effective deployment in the field. Herein, we developed a DNA biosensor platform for the specific and quantitative detection of HIV. The platform contains a rolling circle amplification (RCA)-based DNA biosensor and a portable fluorescence detector, in which HIV-encoded integrase (IN) enzyme activity is used as a biomarker to achieve HIV-specific detection. The cleavage and integration reaction of IN on the sensor surface and RCA are combined in this detection platform to perform detection signal cascade amplification, ultimately achieving a detection limit of 0.125 CFU/μL of HIV particles. Moreover, the DNA sensor system exhibited high sensitivity and accuracy for detecting HIV in clinical samples, suggesting that it has potential for application in clinical settings to detect retroviruses other than HIV. In addition, quantitative detection based on this biosensing platform was significantly correlated with the CD4+ lymphocytes count, which can provide guidance for antiretroviral therapy and which affects long-term death risk assessment in HIV patients. Therefore, this DNA biosensing platform based on IN activity is expected to be useful for rapid HIV testing, diagnosis, and treatment monitoring, enabling the development of new POC diagnostic tests and will thus be highly valuable for developing HIV prevention strategies and effective treatments.

INTRODUCTION

Human immunodeficiency virus (HIV) destroys lymphocytes and causes the body to lose its immune function, leading to acquired immunodeficiency syndrome (AIDS). This virus can persist in the body for years without causing any symptoms.[1,2] Therefore, early and sensitive diagnosis, especially in underdeveloped regions, is an effective strategy for preventing the spread of AIDS. The current diagnostic methods for AIDS mainly rely on HIV antibodies and antigens and include virus neutralization, serological tests, and enzyme-linked immunosorbent assays.[3−5] Due to the low level of HIV antibody in the early stage, these methods have good specificity but lack high sensitivity, making early detection of HIV difficult. In addition, these approaches generally require expensive instruments and equipment, special reagents, professional operators, and exceptionally long analysis times.[6,7] These requirements are increasingly recognized as difficult to meet in underdeveloped and remote epidemic areas and even in cities when epidemics peak. Therefore, there is an urgent need to develop fast, easily operated, low-budget, and portable point-of-care (POC) testing facilities that enable the convenient and timely monitoring of patients for HIV infection in a community or home setting.[8−10]

Received: March 7, 2024
Revised: May 11, 2024
Accepted: May 22, 2024
Published: May 28, 2024

Different sensing strategies for designing POC devices with simple operation, rapid, highly sensitive responses, and quantitative digital results have been assessed in recent years. Enzyme-linked immune sorbent assay (ELISA)-based techniques employing Au nanoparticles[11,12] and DNA barcodes[13] have significantly improved the HIV-1 p24 detection limit to less than 0.5 pg mL^{-1}. Even better results have recently been acquired with pathogen-specific enzyme activity-based DNA biosensors.[14,15] These methods involve directly measuring the activity of microbe-expressed enzymes using various DNA nanosensors. Examples of real-time optical or electrochemical systems for a variety of enzymes relevant to the detection of human diseases such as tuberculosis and cancer[16,17] have been presented. However, most real-time sensors lack adequate sensitivity for real-life diagnosis, and/or their performance is hampered when used to analyze crude biological samples. For diagnostic applications, additional amplification of enzymatic products without hampering the quantitative readout, robustness of the assay, or ease of operation is desirable. One such amplification technique is rolling circle amplification (RCA), in which a circular DNA template is converted to a long tandem repeat RCA product (RCP), which can be visualized at the single-molecule level by using fluorescence (FL) staining or in bulk by using various colorimetric readouts.[18−21] Some notable features, such as isothermal amplification, cost-effectiveness, and high sensitivity, make this technique highly valuable for diagnostic purposes. RCA technology eliminates the precise cyclical heating requirements of qPCR because of its highly efficient continuous synthesis ability and robust strand displacement activity at room temperature. The HIV-encoded integrase (IN) is located in a highly conserved region of the HIV genome with relatively little sequence variation. The selection of the IN gene as the target gene for HIV detection can ensure the specificity of detecting all different subtypes of HIV without being affected by environmental factors. At the same time, it has the advantages of high specificity, strong stability, early diagnosis ability, wide applicability, and drug resistance monitoring. Based on the above characteristics, the single-molecule detection platform developed previously by Wang et al. relies on a DNA biosensor-based RCA technique for sensitive, dose-dependent, and specific detection of HIV-1 and the moloney murine leukemia virus (MLV) in crude biological samples.[22] However, this biosensor can only detect recombinant HIV virus particles (rHIV-1) in crude biological samples and cannot achieve quantitative and qualitative detection of HIV in untreated serum samples from HIV patients. Meanwhile, due to the lack of fast, easily operated, low budget, and portable POC testing facilities, previously developed biosensors were only suitable for laboratory settings and could not conveniently and promptly monitor HIV-infected individuals in POC settings. Therefore, by taking advantage of IN and the low cost and isothermal amplification of RCA technology, we used a modular reaction method to develop a rapid, easy-to-operate, low-budget, and portable single-molecule HIV detection platform that can meet the requirements for a diagnostic application in different scenarios and potentially play a crucial role in AIDS monitoring.[23−33]

Herein, we present a single-molecule detection platform containing a portable FL detector for the readout of an ultrasensitive DNA biosensor chip that allows the selective detection of HIV-1 at a concentration of 0.125 colony-forming units (CFU)/μL. The DNA biosensor has been demonstrated to enable the specific, sensitive, and quantitative detection of purified HIV IN (pHIV-1 IN) and active rHIV-1, which are used as a safe model for HIV. Moreover, the platform demonstrated a potent ability to detect HIV in clinical patient serum samples, with an accuracy of 98.8%, a sensitivity of 99.2%, and a specificity of 98.5%. The biosensing platform can realize rapid on-site diagnosis and screening of HIV, and the quantitative test data are significantly correlated with the CD4 count, which is used in guiding antiretroviral treatment (ART) and in long-term death risk assessment in HIV patients. The current approach represents a significant step forward in the development of a rapid HIV testing platform to enable the ultrasensitive detection of biomarkers, which could have a major impact on public health.

EXPERIMENTAL SECTION

Biosensing Platform Detection of HIV IN. Five femtomoles of 5′amine U5HIV LTR substrate was linked to codelink-activated slides in print buffer overnight in a humidity chamber with saturated NaCl at room temperature. Blocking was carried out for 30 min at 50 °C in a blocking buffer, and the slides were washed twice in ion-exchanged H_2O for 1 min. Subsequently, the slides were washed for 30 min at 50 °C in wash buffer 1, washed twice in ion-exchanged H_2O for 1 min, and air-dried. The U5HIV LTR substrate was generated by hybridization of 5 fmol of a complementary U5HIVB LTR substrate for 30 min at 37 °C in a humified chamber on a hot plate and then washed in wash buffer 2 for 1 min at room temperature and subsequently wash buffer 3 for another 1 min. Finally, the slides were dehydrated in 99.9% ethanol for 1 min and air-dried. Integration reaction assays were performed in 5 μL of a reaction mixture containing 0.5 μL of HIV IN, 50 fmol of 500 bp circle, and 5 fmol of LTR substrate on slides in a reaction buffer. This integrase reaction mixture was incubated for 5 min on ice and then for 2 h at 37 °C. The reaction was stopped by washing in wash buffers 2 and 3 and dehydrated. Rolling circle DNA synthesis was performed in 1 × Phi29 buffer supplemented with 1 μg/μL BSA, 250 μM dNTPs, and 1 unit/μL Phi29 DNA polymerase for 1 h at 37 °C in a humidified chamber on a hot plate. The synthesis reaction was stopped by washing in wash buffers 2 and 3, and the reaction mixture was dehydrated. The RCPs were detected by hybridization to 0.2 μM FAM (green)-labeled probe ID33 and FAM-labeled probe ID A1 in a hybridization buffer. The slides were washed in wash buffers 2 and 3, dehydrated, mounted with Vectashield without DAPI, and placed on glass coverslips. Epifluorescence and bright-field images were captured with a portable FL detector. The detector collects monochromatic emission from each fluorophore and filters it through an appropriate filter. The DNA biosensing platform data system we developed was used for imaging and quantitative FL analysis.

Investigation of the Specificity of the Biosensing Platform. To validate the assay specificity of the biosensing platform, the IN inhibitor raltegravir was used for reverse validation. Raltegravir (MK-0518) is a potent integrase inhibitor against WT and S217Q PFV IN with IC50 values of 90 nM and 40 nM, respectively, in a cell-free assay. It is more than 1000 times more selective for HIV IN than other related Mg^{2+}-dependent enzymes.[34] 0.5 μL of HIV IN, 1 μL of TADA B circle (280 nM), and 0.5, 1, and 2 μL of raltegravir (500 nM/μL) were mixed in 5 μL of reaction buffer separately, incubated on ice for 5 min, then added to the sensor chip coupled with U5HIV LTR substrate and incubated at 37 °C

https://doi.org/10.1021/acsomega.4c02229
ACS Omega 2024, 9, 25042−25053

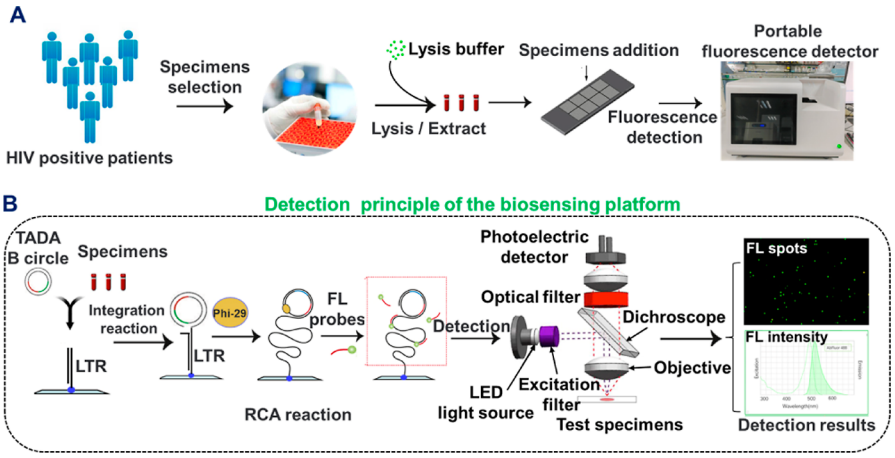

Figure 1. Schematic diagram of the HIV IN-specific DNA biosensing platform based on the RCA technique for multiple amplifications for HIV detection. (A) Flowchart of the detection of serum samples from HIV patients. (B) Detection principle of the biosensing platform. The reaction was performed by adding the double-stranded DNA circle (containing the probe annealing site marked in red) and the test sample containing IN to the slide coupled with the U5 LTR fragment (blue circles). The double-stranded DNA circle is integrated into the slide by IN-mediated LTR fragment cleavage. Upon integration, the double-stranded DNA circle becomes covalently attached to the glass slide, and a free 3′-OH end is generated. Phi-29 polymerase (yellow circle) is added to support the RCA of the uncut strand of the double-stranded DNA circle, generating a long tandem repeat product that can be visualized via a portable FL detector upon hybridization of fluorescently labeled probes. The FL signals generated by the biosensors are analyzed using a portable FL detector. The green FL points represent one RCP generated upon amplification of the product generated by an integration event mediated by HIV IN. A portable FL detector is used to quantitatively analyze the FL intensity of the RCP products.

for 2 h. The reaction was stopped by washing in wash buffers 2 and 3 and dehydrated. Rolling circle DNA synthesis was performed in 1 × Phi29 buffer supplemented with 1 μg/μL BSA, 250 μM dNTPs, and 1 unit/μL Phi29 DNA polymerase for 1 h at 37 °C in a humidified chamber on a hot plate. The synthesis reaction was stopped by washing in wash buffers 2 and 3, and the reaction mixture was dehydrated. The RCPs were detected by hybridization to 0.2 μM FAM (green)-labeled probe ID33 and FAM-labeled probe ID A1 in hybridization buffer. The slides were washed in wash buffers 2 and 3, dehydrated, mounted with Vectashield without DAPI, and placed on glass coverslips. Epifluorescence and bright-field images were captured with a portable FL detector.

Optimization of the Biosensing Platform. We investigated the effects of different RCA primer concentrations, the ratio of TADA B circle to RCA primers, and the concentration of TADA B circle on the detection capability of the biosensing platform. We coupled different concentrations of RCA primers (0, 25, 50, 100, and 200 nM) to the sensor chip, Reaction buffer containing 0.5 μL of HIV IN and 1 μL of TADA B circle (280 nM) was added for integration reaction. After the integration reaction was completed, Phi29 DNA polymerase and FAM-labeled probe ID33 were added sequentially for RCA reaction and FL probe binding reaction. Simultaneously, at a given RCA primer concentration of 100 nM, reaction buffer containing different concentrations of TADA B circle (0, 70, 140, 280, and 560 nM) and 0.5 μL of HIV IN are added to the sensor chip for integration reaction followed by RCA reaction and fluorescence detection. Finally, at a given RCA primer concentration of 100 nM, reaction buffer containing different concentrations of TADA B circle (100, 200, 300, 400, and 500 nM) and 0.5 μL of HIV IN were added to the sensor chip for integration reaction. RCA reactions and FL detection were then performed. The reaction conditions for the integration reaction, RCA reaction, and FL probe binding reaction are the same as described in the specificity investigation section of the biosensing platform.

At the given RCA primer concentration (100 nM) and TADA B circle concentration (300 nM), we gradiently shortened the integration reaction and RCA reaction times to optimize the detection time expenditure of the biosensing platform. The reaction conditions of the integration reaction and RCA reaction were the same as those in the specificity investigation section of the biosensing platform except for time. The reaction conditions for the FL probe binding reaction are the same as described in the specificity investigation section of the biosensing platform.

RESULTS AND DISCUSSION

Design and Working Principle of the Biosensing Platform. The single-molecule detection platform relies on a DNA biosensor-based RCA technique and a portable FL detector (Figure 1) that enables the specific and sensitive testing of clinical serum samples from patients with HIV. We collected and processed serum samples from HIV patients, which were subsequently used in detection with the biosensing platform. The design principle of the DNA biosensor is as follows:[22] first, we designed a double-stranded DNA fragment containing an att site recognized by HIV IN (referred to as the LTR segment). The flanking regions of this segment include two long terminal repeat (LTR) sequences, which are available for binding of HIV IN. The double-stranded DNA circle (TADA B circle) was designed with an identifier sequence identical to the sequence of a fluorescently labeled visualization probe on one strand [termed the (−) strand] and complementary to the sequence of the probe on the other (+) strand. The addition of the IN and TADA B circle to the surface-bound LTR fragment was anticipated to allow the U5 end of the donor to be processed, and the generated recessed 3′-OH end was expected to be integrated into one of the strands of the TADA B circle, followed by the addition of phi-polymerase-generated RCA products that could subsequently be visualized at the single-molecule level upon hybridization to

https://doi.org/10.1021/acsomega.4c02229
ACS Omega 2024, 9, 25042−25053

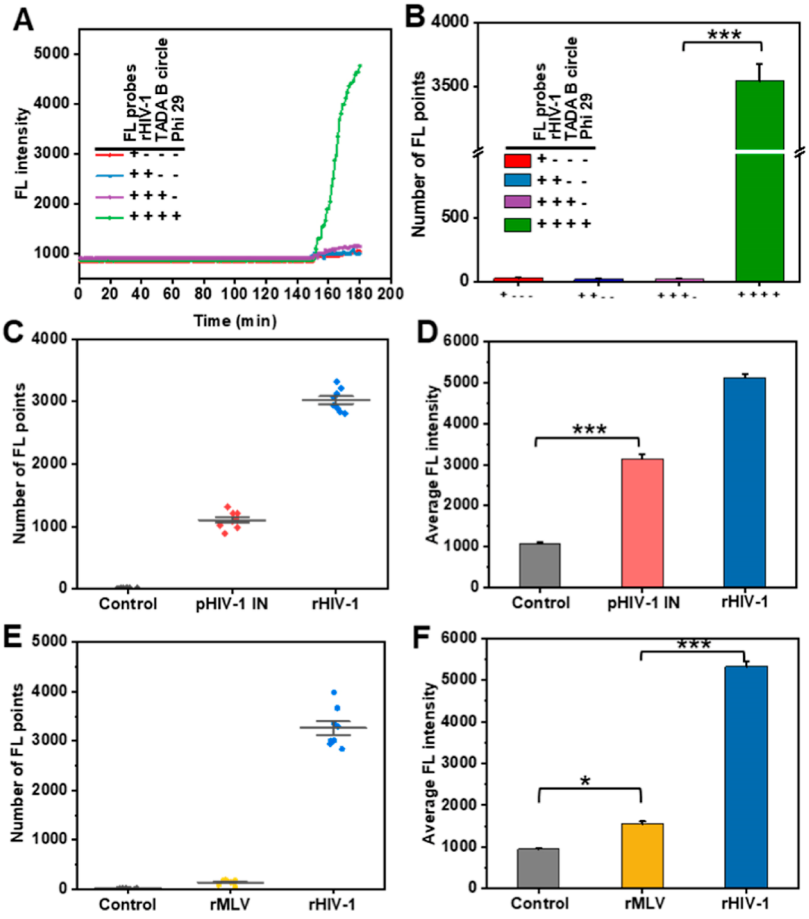

Figure 2. Validation of the specificity and reliability of the biosensing platform. (A) Quantitative plot of the FL intensity of rHIV-1 detected by a portable FL detection system. (B) Bar graph of the counted FL spots detected by the biosensing platform after 180 min of rHIV-1 reaction. (C) Quantitative detection of pHIV-1 IN and rHIV-1 by the biosensing platform. (D) FL intensity quantification graph of pHIV-1 IN and rHIV-1 detected by the biosensing platform. (E) Quantitative detection of rHIV-1 and rMLV by the biosensing platform. (F) FL intensity quantification graph of rHIV-1 and rMLV detected by the biosensing platform. Error bars were generated from 3 independent replicates. Data were normalized against the average obtained from 10 random images obtained in each repetition. The error bars represent the standard error of the mean of the indicated three independent experiments. *P < 0.05, **P < 0.01, ****P < 0.0001.

the fluorescently labeled visualization probes. Then, our independently developed portable FL detector and data processing system were utilized to detect and analyze the FL signals generated by the reaction. The enzymatic integration reaction signals were directly transformed into visualized and quantified FL signals to achieve accurate detection of clinical serum samples of HIV patients.

Validation of the Biosensing Platform. To validate the detection capability of the biosensing platform, we first performed direct detection of rHIV-1. After lysis, the rHIV-1 were directly added to the DNA biosensor for reaction. We measured the FL intensity every 1 min throughout the reaction period using a portable FL detector. The rHIV-1, TADA B-Circle, phi29 DNA polymerase, and fluorescent probes were individually added to the biosensor system for the reaction. The FL intensity results revealed a background FL of less than 1000 au; however, when all of the above four substances were added to the reaction system, significant amounts of FL were generated compared with that in the control group. Interestingly, after RCA was completed, the addition of the fluorescent probe to the biosensor system without phi29 DNA polymerase resulted in a higher background FL in the group, possibly due to nonspecific adsorption of the FL probe on the functionalized glass slides (Figure 2A). Moreover, we performed quantitative statistics on the number of FL points in the four groups (Figure 2B). These preliminary validation results showed that our DNA biosensor could enable rHIV-1 detection.

Next, we further evaluated the specificity of the biosensor platform we developed by using pHIV-1 IN, rHIV-1, and recombinant moloney murine leukemia virus (rMLV). We added 10 ng/μL pHIV-1 IN and 125 CFU of rHIV-1 to the biosensor platform for detection. The quantitative results of FL intensity and FL spot numbers showed that both the pHIV-1 IN group and the rHIV-1 group produced strong FL signals compared to those in the control group (Figure 2C,D). Additionally, to assess the ability of the biosensor platform to distinguish similar RNA viruses, 125 CFU of rMLV was added to reaction slides modified with the U5HLV LTR substrate, after which the FL intensity and spot number were detected using the portable FL detector. The results revealed that only a small number of signals in the samples with added rMLV were stronger than the background, indicating that our single-molecule-scale DNA biosensor platform can accurately identify HIV IN for specific HIV detection (Figure 2E,F).

Investigation of the Sensitivity and Specificity of the Biosensing Platform. To evaluate the sensitivity and specificity of the HIV single-molecule detection biosensing

https://doi.org/10.1021/acsomega.4c02229
ACS Omega 2024, 9, 25042−25053

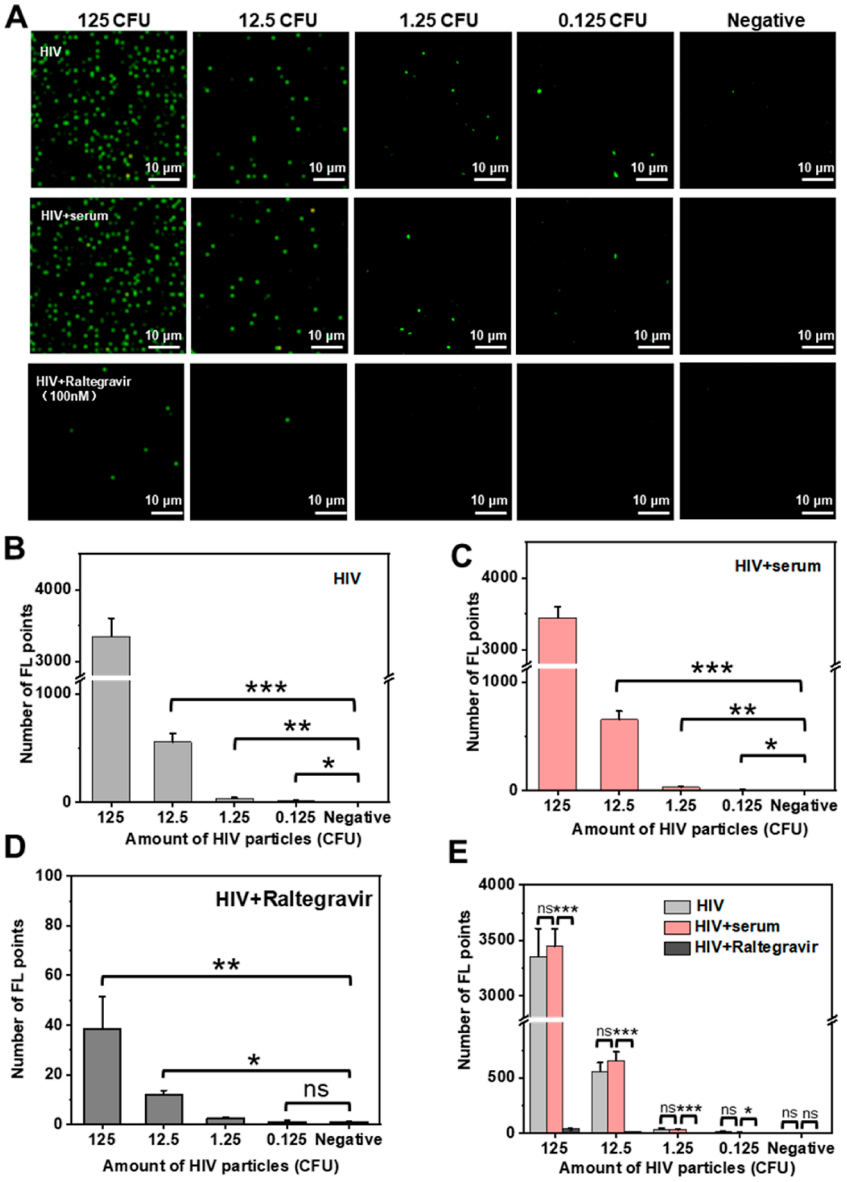

Figure 3. Evaluation of the sensitivity and specificity of the biosensing platform. (A) FL imaging of rHIV-1after different treatments. (B) Quantitative detection results of FL points at different concentrations of HIV. (C) Quantitative detection of FL spots at different concentrations in HIV + serum. (D) Statistical analysis of the quantitative results of FL points at different concentrations of HIV + raltegravir. (E) Comparative quantitative results of FL points between the HIV group, HIV + serum group, and HIV + raltegravir group. The scale bar represents 10 μm. The number of virus particles is stated in CFU corresponding to 25 virus particles per μL in the initial sample. The error bars represent the standard error of the mean of the indicated three independent experiments. *P < 0.05, **P < 0.01, ****P < 0.0001.

platform for HIV detection, we prepared simulated patient samples from engineered rHIV-1 with defects cultured in a cell culture medium containing 10% fetal bovine serum. Extracts obtained from gradient-diluted defective rHIV-1 were added to the detection system for the reaction. Under conditions of 37 °C, HIV IN integration for 50 min, and RCA for 30 min, fluorescence microscopy images based on the developed single-molecule detection platform were obtained for rHIV-1 at the concentrations of 125 CFU, 12.5 CFU, 1.25 CFU, and 0.125 CFU, as shown in Figure 3A. Each rHIV-1 group exhibited strong FL signals, while the virus-free group showed no FL signal and only a minimal background FL signal. The FL spot signals obtained from the portable FL detection data analysis system were 3355 + 252.4, 557 + 78.3, 37 + 8.5, and 13 + 2.6 (Figure 3B). The detected FL signals decreased gradually with decreasing quantity of HIV viruses in the samples. The average FL signal of the negative control group (2 + 1.0) plus three times its standard deviation was set as the positive threshold (cutoff value = 4). The HIV single-molecule detection platform achieved a minimum detection limit of 0.125 CFU/μL for packaged HIV particles, which was significantly lower than that of the FL spots in the negative control group (P < 0.05). Notably, the samples used for HIV testing are typically serum isolated from blood samples of suspected patients. To exclude the interference of various biological samples on the detection performance of the system and to verify the potential of this DNA biosensing platform in future diagnostic applications, we used a human serum test detection device to assess specificity and sensitivity. We mixed viruses generated from cell cultures with human serum extracts

https://doi.org/10.1021/acsomega.4c02229
ACS Omega 2024, 9, 25042−25053

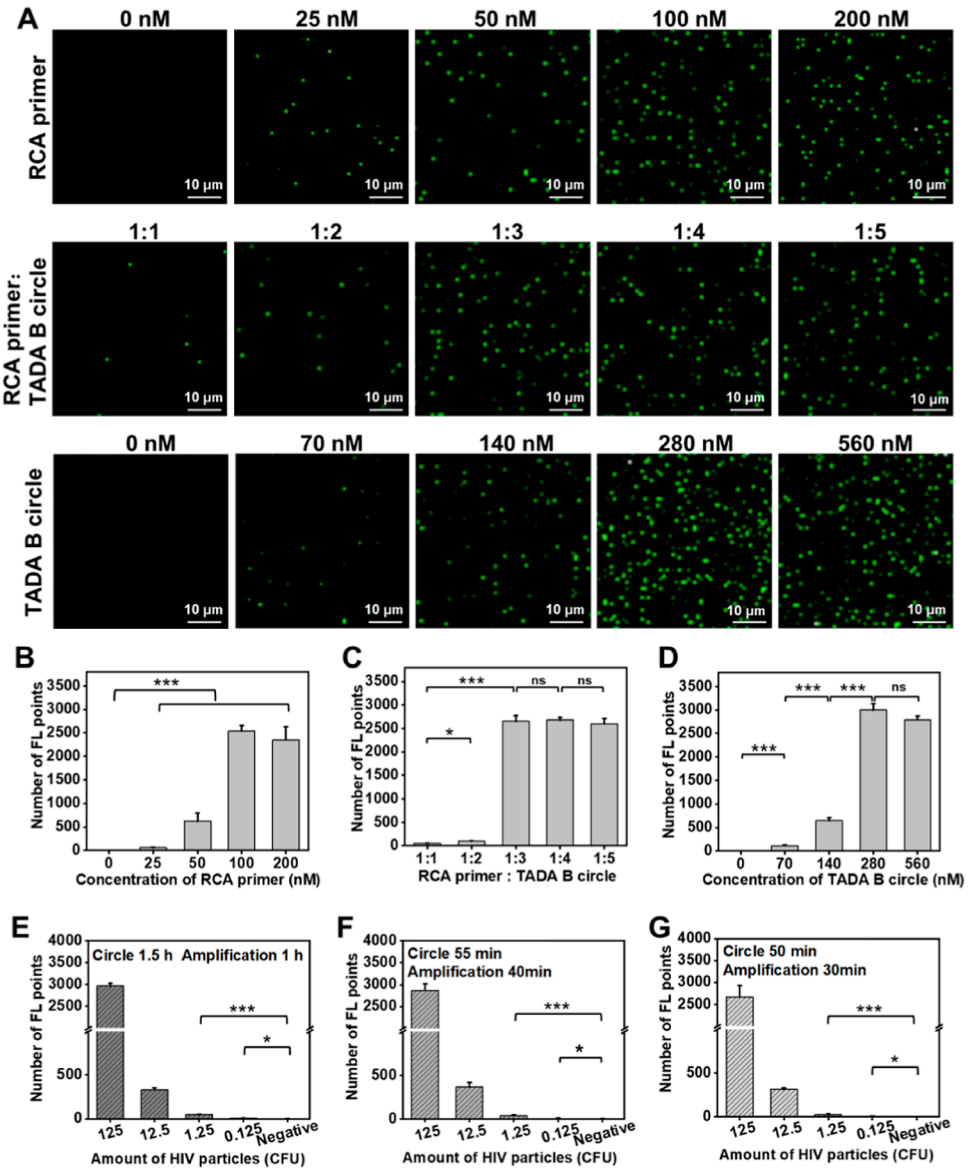

Figure 4. Biosensing platform optimization scheme. (A) FL imaging of the single-molecule HIV detection biosensing platform under different parameter conditions. Scale bars: 10 μm. (B) Relationships between the RCA primer concentration and the FL signal. (C) Effect of the RCA primer:TADA B circle ratio on the FL signal. (D) Investigation of the effect of the TADA B-cell concentration on the FL signal of the biosensing platform. (E) Quantitative statistical plot of circle cyclization for 1.5 h and RCA for 1 h. (F) Quantitative statistical plot of circle cyclization for 55 min and RCA for 40 min. (G) Quantitative statistical plot of circle cyclization for 50 min and RCA for 30 min. The scale bar represents 10 μm. The number of virus particles is stated in CFU corresponding to 25 virus particles per μL in the initial sample. The error bars represent the standard error of the mean of the indicated three independent experiments. *P < 0.05, **P < 0.01, ****P < 0.0001.

for system testing, FL readings, and quantitative analysis. There was no significant difference in the number of FL spots between the signals from HIV alone and those from the addition of human serum (Figure 3C). The FL spot signals in the rHIV-1 group with serum were not significantly different from those in the rHIV-1 group without serum (P > 0.05) (Figure 3E). These results further indicate that various complex components in serum samples have little effect on the detection of HIV RNA. Simultaneously, we conducted a series of tests to determine the influence of sample processing and storage conditions. By testing positive and negative simulated patient samples, we found a nonlinear relationship between the concentration of rHIV-1 and the quantity of FL signals. The exact cause of this nonlinearity remains unclear and may be related to the degree of aggregation among the HIV IN monomers.

To validate the specificity of the HIV single-molecule detection biosensing platform, reverse validation was performed using the IN inhibitor raltegravir. We selected concentrations of 50 nM, 100 nM, and 200 nM to assess the reliability of the single-molecule detection platform. At 37 °C, with HIV IN integration for 50 min and RCA for 30 min, 50 nM, 100 nM, or 200 nM raltegravir was added to the DNA sensor along with 125 CFU rHIV-1 for detection. FL imaging revealed a strong signal in the 50 nM raltegravir group, while the signals in the 100 nM and 200 nM raltegravir groups were very weak. The blank control group exhibited the highest FL signal, indicating that treatment with raltegravir at concentrations of 100 nM and 200 nM completely inhibited the IN

https://doi.org/10.1021/acsomega.4c02229
ACS Omega 2024, 9, 25042−25053

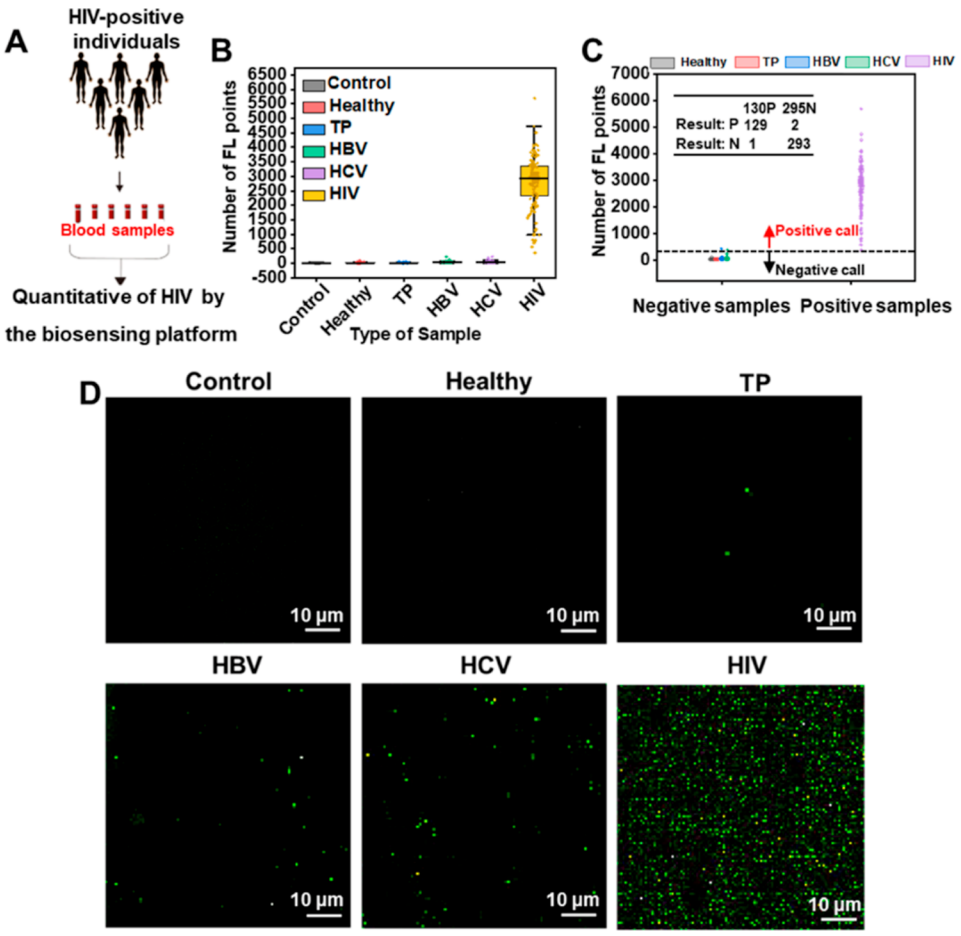

Figure 5. Biosensing platform detects HIV in human serum samples. (A) Schematic representation of serum sample collection from HIV-positive patients. (B) Quantitative statistics of FL spots in the biosensing platform detection of HIV-positive patient serum samples. (C) Threshold statistics of FL spots in the biosensing platform for detecting HIV-positive and HIV-negative samples. (D) FL imaging of healthy individual serum specimens, TP patient serum specimens, HBV patient serum specimens, HCV patient serum specimens, and HIV patient serum specimens for detection via the biosensing platform. The scale bar represents 10 μm.

activity of 125 CFU rHIV-1 (Figure S1). Subsequent experiments were conducted using 100 nM raltegravir.

Next, 100 nM raltegravir was mixed with HIV particles packaged with different concentration gradients and added to the DNA biosensing platform for reaction. The FL imaging results revealed a significant reduction in FL signals upon the addition of raltegravir, with only the 125 CFU and 12.5 CFU groups exhibiting faint FL signals (Figure 3A). This reduction may be attributed to the inhibitory effect of raltegravir on the integration of HIV IN at the DNA nanosensor interface. The HIV + raltegravir group displayed FL spot signals of 38 + 13.2, 12 + 1.6, 3 + 0.6, and 1 + 0.0. This result confirmed the excellent specificity of the HIV single-molecule biosensor platform based on HIV IN detection (Figure 3D,E).

Optimization of the Biosensing Platform. To achieve optimal detection, a series of parameters affecting the detection capability of the RCA-based DNA sensor system, including the RCA primer concentration, the ratio of the TADA B circle to the RCA primer, and the concentration of the TADA B circle, were systematically investigated (Figure 4). As expected, the FL signals increased with increasing RCA primer concentrations (Figure 4A,B). When the RCA primer concentration exceeded 40 nM/μL, the FL signals slightly decreased with increasing RCA primer concentration, possibly because of the covalent attachment of two or more primer fragments when a large excess of RCA primer was incubated with the TADA B gene. Thus, 40 nM was selected as the concentration of RCA primers for subsequent experiments. The TADA B circle serves as a template for RCA reactions, and its concentration may greatly affect the FL signal yield of the DNA sensor system. As shown in (Figure 4A,C), higher concentrations of TADA B led to higher FL output signals, with a plateau at 3-fold. Moreover, at an RCA primer concentration of 100 nM, after 120 min of cleavage and ligation, higher concentrations of the TADA B circle led to significantly greater FL signals than did lower concentrations of the TADA B circle or the absence of the TADA B circle. When the TADA B concentration was 280 nM/μL, the FL signals of the RCPs reached a plateau (Figure 4A,D). Therefore, 280 nM TADA B was chosen for HIV IN detection in the HIV single-molecule detection platform. The optimized parameters mentioned above were used for subsequent experiments.

Simultaneously, to meet the requirements of on-site rapid detection, the incubation time of IN and the RCA amplification time in the HIV single-molecule detection biosensing platform were optimized. The RCA primers generated by the cleavage and integration of the TADA B circle by HIV IN were used to determine whether the subsequent RCA reaction could proceed smoothly; the FL signal is related to the incubation time, so the RCPs resulting

https://doi.org/10.1021/acsomega.4c02229
ACS Omega 2024, 9, 25042−25053

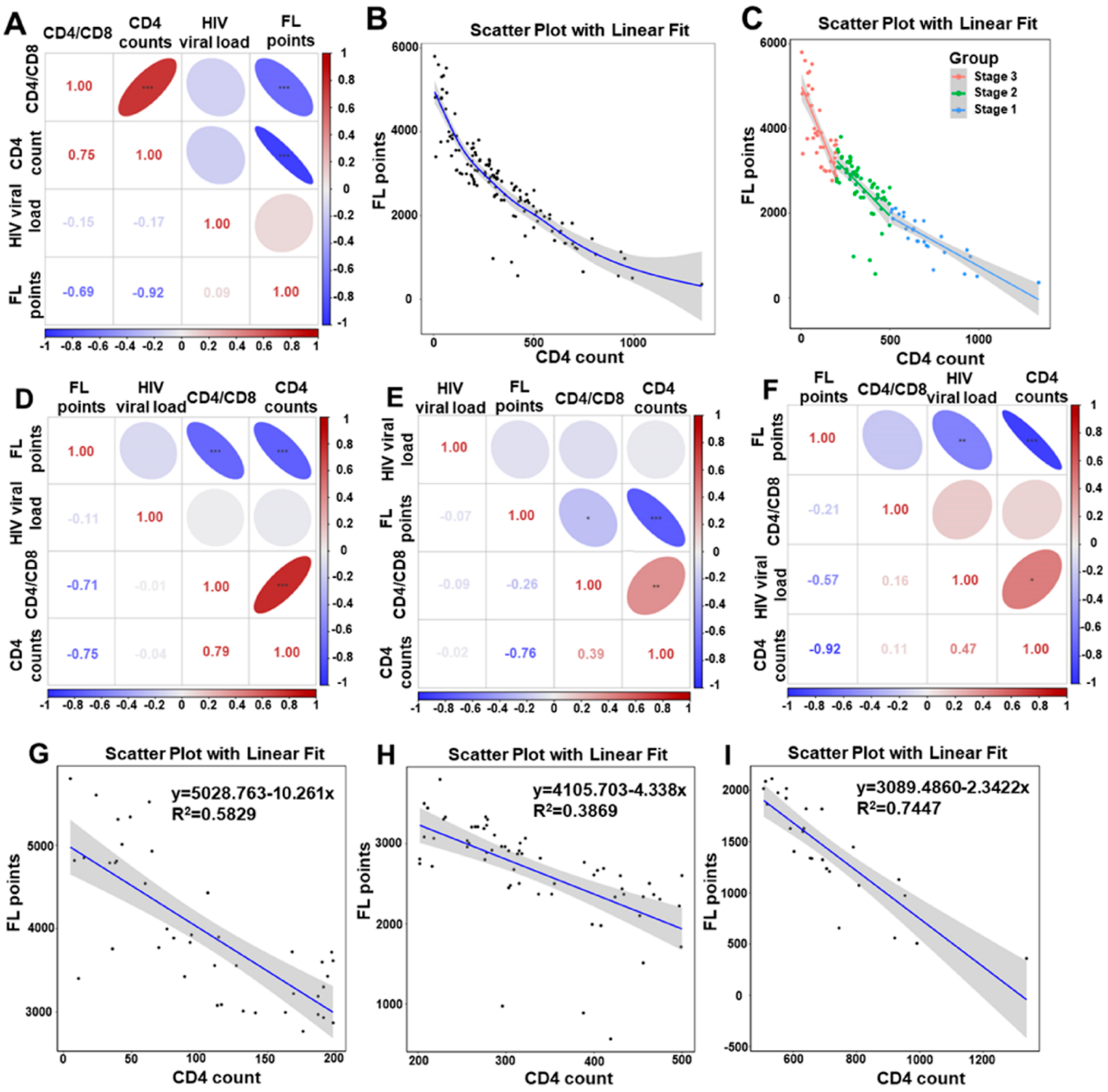

Figure 6. Relationships between various clinical indicators and HIV infection. (A) Spearman correlation coefficient image between laboratory markers related to HIV infection. (B) Analysis of the nonlinear fit of the FL readings and CD4+ lymphocyte count. (C) Linear fit analysis images of FL readings and CD4+ lymphocyte counts in 130 patients. (D−F) Images of Spearman correlation coefficients of laboratory markers associated with HIV infection in patients at different stages. (G−I) Linear fit analysis images of FL readings and CD4+ lymphocyte counts of patients at different stages.

from different incubation times were examined. The reaction time of HIV IN integration was shortened from 2 to 1.5 h, and the reaction time of RCA isothermal amplification was unchanged. Compared with the experimental results obtained under the optimized reaction conditions, the FL intensity and number of FL spots did not change significantly under the optimized reaction conditions. Shortening the integration reaction time of HIV IN by 0.5 h did not affect the sensitivity of HIV-specific detection (Figure 4E). The integration reaction time of HIV IN was further reduced from 2 h to 55 min, and the isothermal amplification reaction time of RCA was further shortened from 1 h to 40 min. Compared to the experimental results obtained under nonoptimized reaction conditions, there was no significant change in the FL intensity or number of FL spots under the optimized conditions. This finding indicates that HIV-specific detection can be achieved with an incubation time of 55 min for HIV IN and an isothermal amplification time of 40 min for RCA without compromising the detection sensitivity (Figure 4F). The reaction time of HIV IN integration further decreased from 2 h to 50 min, and the reaction time of RCA isothermal amplification decreased from 1 h to 30 min. Compared with the experimental results obtained under the nonoptimized reaction conditions, the FL intensity and FL amount under the optimized reaction

https://doi.org/10.1021/acsomega.4c02229
ACS Omega 2024, 9, 25042−25053

conditions also did not change significantly ($P > 0.05$) (Figure 4G). Therefore, HIV IN integration for 50 min and RCA isothermal amplification for 30 min were used as the final parameters for subsequent clinical sample testing. The optimization procedure greatly shortened the detection time and improved the detection efficiency of samples without reducing the HIV detection sensitivity.

Detection of HIV within Clinical Samples by the Biosensing Platform. Under the optimal conditions, clinical serum samples from known HIV-infected individuals with positive or negative RT−PCR results were tested using the HIV biosensing platform. A total of 130 serum samples from individuals at different clinical stages of HIV infection were collected and processed. Based on the CDC criteria,[35] 42 (32%), 62 (48%), and 26 (20%) patients were assigned to stages 1, 2, and 3, respectively (Table S1). Fifty (38%) patients had not previously received ART. All patients were treated with a regimen that included at least one nucleoside reverse transcriptase inhibitor (NRTI) [Zidovudine, Lamivudine, Tenofovir, Abacavir, Didanosine, Stavudine]. Thirty-two patients (25%) received a regimen containing the nonnucleoside reverse transcriptase inhibitor (NNRTI) [Efavirenz, Nevirapine], and fifty-nine patients (22%) received a regimen containing protease inhibitor (PI) drugs [lopinavir/ritonavir, Kaletra] (Table S2). The mean CD4 counts among patients with stage 1, 2, and 3 disease were 447.2, 399.1, and 127.5 cells per cubic millimeter, respectively. The mean viral load was 22,041 in patients with stage 1 disease, 10,845 in patients with stage 2 disease, and 49,207 in patients with stage 3 disease. Additionally, serum samples from 55 syphilis-infected (TP) patients, 55 hepatitis B-infected (HBV) patients, 55 hepatitis C-infected (HCV) patients, and 130 healthy individuals undergoing medical examinations were collected as a control group to validate the specificity of the HIV biosensing platform and explore whether common clinical RNA viruses would cause false-positive interference with the DNA sensor detection (Figure 5A). Clinical serum sample information is given in Tables S2−S6. The FL imaging results of patient serum samples detected by the biosensing platform are shown in Figure 5D. FL signals were detected in 130 clinical serum samples from HIV-positive patients, with one serum sample from a patient whose DNA biosensor test result was a false negative. The abnormal samples were from patients with HBV infection, and the test results were relatively significantly different from those of the HIV-positive samples ($p < 0.05$). As depicted in Figure 5B, there were significant differences in the FL signals between the 129 patient samples and the 130 healthy individual samples ($p < 0.001$), as well as between the patient samples and the negative control, demonstrating the ability of the sensor system to effectively discriminate HIV-positive samples from negative samples (Figure 5B). To determine infection using the biosensing platform, we derived a threshold of 300 FL signals based on the current results. Based on the detection threshold, the clinical samples from TP patients and healthy individuals showed similar signals, all of which were below the threshold. In contrast, clinical samples from HBV and HCV patients each exhibited one abnormal signal above the threshold. Therefore, according to the detection threshold, the calculated accuracy, sensitivity, and specificity of the DNA biosensing platform for detecting HIV in patient serum samples were 98.8, 99.2, and 98.5%, respectively. However, further studies involving a larger number of patients may be necessary to establish a more accurate threshold for even more sensitive and specific detection of HIV infections (Figure 5C). The results showed that the optimized HIV biosensing platform could identify almost all clinical serum samples of HIV patients sensitively, specifically, and accurately and could exclude interference from clinical samples of similar RNA viruses.

Correlation Analysis between FL Readings and Various Clinical Indicators. We explored the relationship between laboratory parameters related to HIV infection at different stages of the disease. For each patient, the number of FL readings, number of T-CD4 lymphocytes and HIV-1 viral load were assessed. Figure 6A shows the Spearman correlation coefficients for the clinical sample parameters for the 130 HIV patients. Although an inverse correlation between CD4 counts and HIV-1 RNA levels was observed in previous studies,[36,37] this correlation was not evident in our study. The assessment of changes in the plasma HIV RNA level and CD4+ lymphocyte count over the course of the disease revealed no relationship between the plasma HIV RNA level and the CD4+ lymphocyte count over time. However, we found that the FL readings from the biosensing platform did correlate significantly with the patient's CD4+ lymphocyte count and the ratio of CD4+ to CD8+ lymphocytes. As shown in Figure 6A, as the CD4+ lymphocyte count and the ratio of CD4+ to CD8+ lymphocytes increased, the number of FL points measured by the biosensing platform decreased, indicating a negative correlation. Linear fits of the CD4+/CD8+ lymphocytes to the FL data are shown in Figure S2. This finding suggested that, in addition to HIV RNA levels, FL measurements can play a guiding role in the management of ART. T-CD4+ cells are the most important cell line affected by HIV. Since CD4 lymphocytes are the first to be affected by the virus and their number rapidly decreases as the disease progresses, the measurement of the CD4 count is an important indicator for assessing the effectiveness of treatments and disease progression. Therefore, we further employed the gam function to perform a nonlinear fitting of the CD4+ lymphocyte count and FL readings in HIV patients. The R^2 of the nonlinear fitting curve was 0.749, p value < 0.001, indicating statistically significant evidence of nonlinearity between the FL readings and the CD4+ lymphocyte count. Moreover, we analyzed the correlation between various experimental parameters in serum samples from stage 1, stage 2, and stage 3 patients according to the CDC staging criteria. As shown in Figure 6D−F, the Spearman correlation coefficients indicated that, in addition to a significant correlation between the CD4+ lymphocyte count and FL, there are also correlations between the HIV RNA level and FL, as well as between the CD4+ lymphocyte count, in stage 1 patients. This result may be related to the strength of HIV replication activity in patients at different stages. FL readings based on integrase activity measurements tend to represent replication-active viruses in vivo. Considering the nonsignificance of these nonlinear tests, we conducted linear fitting of CD4+ lymphocyte counts and FL readings for patients at different stages according to the CDC staging criteria. The p values for the linear relationships were all <0.001, indicating a statistically significant correlation between FL readings and CD4+ lymphocyte count. In conclusion, our biosensing platform not only enables rapid diagnosis of HIV patients but also serves as an auxiliary tool for assessing and monitoring their health status. Integrating FL readings with patient age, BMI, socioeconomic factors, treatment modalities, and other health issues holds significance in predicting long-

https://doi.org/10.1021/acsomega.4c02229
ACS Omega 2024, 9, 25042−25053

term mortality risk in patients. This can serve as a crucial indicator of treatment efficacy and disease progression.

CONCLUSIONS

A DNA biosensing platform based on HIV IN activity and RCA technology was designed for the ultrasensitive detection of HIV. The personalized and controllable synthesis of DNA substrates in the RCA-based biosensing system makes this system highly adaptable, allowing alternative types of enzyme cleavage−ligation reactions or modifications of other kinds of oligonucleotides on slides and thus offering broad application prospects. Moreover, an RCA-based cascade amplification strategy was used to generate a large amount of output DNA, which can link abundant DNA fluorescent probes to RCPs, generating significantly amplified signals for sensitive analysis of HIV. In fact, a small volume (5 μL) of the analyzed sample was shown to be sufficient for the DNA biosensor to reliably deliver stable FL output signals for sufficient time to acquire a digital measurement. Interestingly, this single-molecule detection platform detects the presence of HIV particles at a concentration of 0.125 CFU/μL, which is promising for the POC-based diagnosis of early-stage HIV-1 infection. This work not only developed a novel DNA biosensor but also provided a multifunctional portable FL signal detector, which holds promise as a biosensor for the rapid and accurate detection of HIV and has been effectively applied in real human serum samples. The biosensing platform can realize rapid on-site diagnosis and screening of HIV, and the quantitative test data are significantly correlated with the CD4+ lymphocytes count, which has a certain guiding role in ART treatment and in long-term death risk assessment in HIV patients. To provide a decentralized approach to diagnostics, the proposed single-molecule detection platform is a crucial development and could present new opportunities in the field of ultrasensitive POC testing, particularly in rural locations.

ASSOCIATED CONTENT

Supporting Information

The Supporting Information is available free of charge at https://pubs.acs.org/doi/10.1021/acsomega.4c02229.

Details about materials, construction of recombinant plasmid DNA for HIV IN, construction of TADA B circle, expression and purification of HIV IN, Western blot analysis for HIV IN, collection and processing of clinical specimens, and parameter configuration of the portable FL detector, FL imaging of recombinant HIV-1, linear fit analysis, CD4 count based on CDC classification, clinical and demographic characteristics of 130 patients and healthy people in this study, clinical and demographic characteristics of 55 patients with HBV, 55 patients with HCV, and 55 patients with TP in this study (PDF)

AUTHOR INFORMATION

Corresponding Authors

Feng Wang − *Shenzhen Center for Chronic Disease Control, Shenzhen Institute of Dermatology, Shenzhen 518020, China*; Email: biowangfeng@163.com

Zhengrong Yang − *Shenzhen Pingshan Center for Disease Control and Prevention, Shenzhen 518118, China*; Email: yangzr@szcdc.net

Furong Li − *Translational Medicine Collaborative Innovation Center, The First Affiliated Hospital (Shenzhen People's Hospital), Southern University of Science and Technology, Shenzhen 518055, China; GuangDong Engineering Technology Research Center of Stem Cell and Cell Therapy, Shenzhen Key Laboratory of Stem Cell Research and Clinical Transformation, Shenzhen Immune Cell Therapy Public Service Platform, Shenzhen 518020, China; Institute of Health Medicine, Southern University of Science and Technology, Shenzhen 518055, China*; orcid.org/0009-0002-7993-1133; Email: lifurong@mail.sustech.edu.cn

Authors

Fuming Chen − *Translational Medicine Collaborative Innovation Center, The First Affiliated Hospital (Shenzhen People's Hospital), Southern University of Science and Technology, Shenzhen 518055, China; GuangDong Engineering Technology Research Center of Stem Cell and Cell Therapy, Shenzhen Key Laboratory of Stem Cell Research and Clinical Transformation, Shenzhen Immune Cell Therapy Public Service Platform, Shenzhen 518020, China*

Jing Wang − *Translational Medicine Collaborative Innovation Center, The First Affiliated Hospital (Shenzhen People's Hospital), Southern University of Science and Technology, Shenzhen 518055, China; GuangDong Engineering Technology Research Center of Stem Cell and Cell Therapy, Shenzhen Key Laboratory of Stem Cell Research and Clinical Transformation, Shenzhen Immune Cell Therapy Public Service Platform, Shenzhen 518020, China*

Jie Ma − *Translational Medicine Collaborative Innovation Center, The First Affiliated Hospital (Shenzhen People's Hospital), Southern University of Science and Technology, Shenzhen 518055, China; GuangDong Engineering Technology Research Center of Stem Cell and Cell Therapy, Shenzhen Key Laboratory of Stem Cell Research and Clinical Transformation, Shenzhen Immune Cell Therapy Public Service Platform, Shenzhen 518020, China*

Li Song − *Translational Medicine Collaborative Innovation Center, The First Affiliated Hospital (Shenzhen People's Hospital), Southern University of Science and Technology, Shenzhen 518055, China; GuangDong Engineering Technology Research Center of Stem Cell and Cell Therapy, Shenzhen Key Laboratory of Stem Cell Research and Clinical Transformation, Shenzhen Immune Cell Therapy Public Service Platform, Shenzhen 518020, China*

Haojie Yan − *Translational Medicine Collaborative Innovation Center, The First Affiliated Hospital (Shenzhen People's Hospital), Southern University of Science and Technology, Shenzhen 518055, China; GuangDong Engineering Technology Research Center of Stem Cell and Cell Therapy, Shenzhen Key Laboratory of Stem Cell Research and Clinical Transformation, Shenzhen Immune Cell Therapy Public Service Platform, Shenzhen 518020, China*

Complete contact information is available at: https://pubs.acs.org/10.1021/acsomega.4c02229

Author Contributions

F.C.: Methodology, software, collection and testing of samples, writing-original draft preparation; J.W.: Conceptualization; J.M.: Biosensing platform optimization; L.S.: Providing serum samples of healthy individuals and HBV/HCV patients; H.-

https://doi.org/10.1021/acsomega.4c02229
ACS Omega 2024, 9, 25042−25053

J.Y.: Investigation; F.W.: Providing serum samples of TP patients; Z.Y.: Providing serum samples of HIV patients; F.L.: Supervision, writing- reviewing and editing. All authors read and approved the final manuscript.

Notes

The authors declare no competing financial interest.

■ ACKNOWLEDGMENTS

The work was supported by the Shenzhen Science and Technology Program (grant numbers GJHZ20190821161420866), the National Natural Science Foundation of China (grant number 82001755), the Shenzhen Science and Technology Program (JCYJ20190807144609346), and the Natural Science Foundation of Guangdong Province (grant number 2020A1515110521).

■ ABBREVIATIONS

POC, point-of-care; HIV, human immunodeficiency virus; RCA, rolling circle amplification; FL, fluorescence; ART, antiretroviral therapy; AIDS, acquired immunodeficiency syndrome; RCP, rolling circle amplification product; LTR, long terminal repeat sequences

■ REFERENCES

(1) Dabis, F.; Bekker, L.-G. We still need to beat HIV. *Science* **2017**, *357* (6349), 335.

(2) Ma, Y.; Shen, X.-L.; Zeng, Q.; Wang, H.-S.; Wang, L.-S. A multi-walled carbon nanotubes based molecularly imprinted polymers electrochemical sensor for the sensitive determination of HIV-p24. *Talanta* **2017**, *164*, 121−127.

(3) Du, M.; Li, N.; Mao, G.; Liu, Y.; Wang, X.; Tian, S.; Hu, Q.; Ji, X.; Liu, Y.; He, Z. Self-assembled fluorescent Ce(III) coordination polymer as ratiometric probe for HIV antigen detection. *Anal. Chim. Acta* **2019**, *1084*, 116−122.

(4) Miller, B. S.; Thomas, M. R.; Banner, M.; Kim, J.; Chen, Y.; Wei, Q.; Tseng, D. K.; Göröcs, Z. S.; Ozcan, A.; Stevens, M. M.; McKendry, R. A. Sub-picomolar lateral flow antigen detection with two-wavelength imaging of composite nanoparticles. *Biosens. Bioelectron.* **2022**, *207*, 114133.

(5) Li, J.; Wang, J.-L.; Zhang, W.-L.; Tu, Z.; Cai, X.-F.; Wang, Y.-W.; Gan, C.-Y.; Deng, H.-J.; Cui, J.; Shu, Z.-C.; Long, Q.-X.; Chen, J.; Tang, N.; Hu, X.; Huang, A.-L.; Hu, J.-L. Protein sensors combining both on-and-off model for antibody homogeneous assay. *Biosens. Bioelectron.* **2022**, *209*, 114226.

(6) Tosiano, M. A.; Mar, H.; Hoeth, D.; Eron, J. J.; Gandhi, R. T.; McMahon, D. K.; Bosch, R. J.; Mellors, J. W.; Cyktor, J. C. Comparative sensitivity of automated (Abbott M2000) and manual plasma HIV-1 RNA PCR assays for the detection of persistent viremia after long-term antiretroviral therapy. *J. Virus Erad.* **2022**, *8* (4), 100095.

(7) McFall, S. M.; Wagner, R. L.; Jangam, S. R.; Yamada, D. H.; Hardie, D.; Kelso, D. M. A simple and rapid DNA extraction method from whole blood for highly sensitive detection and quantitation of HIV-1 proviral DNA by real-time PCR. *J. Virol. Methods* **2015**, *214*, 37−42.

(8) Brendish, N. J.; Poole, S.; Naidu, V. V.; Mansbridge, C. T.; Norton, N. J.; Wheeler, H.; Presland, L.; Kidd, S.; Cortes, N. J.; Borca, F.; Phan, H.; Babbage, G.; Visseaux, B.; Ewings, S.; Clark, T. W. Clinical impact of molecular point-of-care testing for suspected COVID-19 in hospital (COV-19POC): a prospective, interventional, non-randomised, controlled study. *Lancet Respir. Med.* **2020**, *8* (12), 1192−1200.

(9) Qi, L.; Yang, M.; Chang, D.; Zhao, W.; Zhang, S.; Du, Y.; Li, Y. A DNA Nanoflower-Assisted Separation-Free Nucleic Acid Detection Platform with a Commercial Pregnancy Test Strip. *Angew. Chem., Int. Ed.* **2021**, *60* (47), 24823−24827.

(10) Hao, L.; Yang, W.; Xu, Y.; Cui, T.; Zhu, G.; Zeng, W.; Bian, K.; Liang, H.; Zhang, P.; Zhang, B. Engineering light-initiated afterglow lateral flow immunoassay for infectious disease diagnostics. *Biosens. Bioelectron.* **2022**, *212*, 114411.

(11) Banerjee, R.; Jaiswal, A. Recent advances in nanoparticle-based lateral flow immunoassay as a point-of-care diagnostic tool for infectious agents and diseases. *Analyst* **2018**, *143* (9), 1970−1996.

(12) Yang, W.; Li, X.-b.; Liu, G.-w.; Zhang, B.-b.; Zhang, Y.; Kong, T.; Tang, J.-j.; Li, D.-n.; Wang, Z. A colloidal gold probe-based silver enhancement immunochromatographic assay for the rapid detection of abrin-a. *Biosens. Bioelectron.* **2011**, *26* (8), 3710−3713.

(13) Marsden, M. D.; Zhang, T.-h.; Du, Y.; Dimapasoc, M.; Soliman, M. S. A.; Wu, X.; Kim, J. T.; Shimizu, A.; Schrier, A.; Wender, P. A.; Sun, R.; Zack, J. A. Tracking HIV Rebound following Latency Reversal Using Barcoded HIV. *Cell Rep. Med.* **2020**, *1* (9), 100162.

(14) Mota, D. S.; Guimaraes, J. M.; Gandarilla, A. M. D.; Filho, J.; Brito, W. R.; Mariúba, L. Recombinase polymerase amplification in the molecular diagnosis of microbiological targets and its applications. *Can. J. Microbiol.* **2022**, *68* (6), 383−402.

(15) Lillis, L.; Lehman, D. A.; Siverson, J. B.; Weis, J.; Cantera, J.; Parker, M.; Piepenburg, O.; Overbaugh, J.; Boyle, D. S. Cross-subtype detection of HIV-1 using reverse transcription and recombinase polymerase amplification. *J. Virol. Methods* **2016**, *230*, 28−35.

(16) Xu, S.; Wang, X.; Wu, C.; Zhu, X.; Deng, X.; Wu, Y.; Liu, M.; Huang, X.; Wu, L.; Huang, H. MscI restriction enzyme cooperating recombinase-aided isothermal amplification for the ultrasensitive and rapid detection of low-abundance EGFR mutations on microfluidic chip. *Biosens. Bioelectron.* **2024**, *247*, 115925.

(17) Zhang, Y.; Chen, S.; Ma, J.; Zhou, X.; Sun, X.; Jing, H.; Lin, M.; Zhou, C. Enzyme-catalyzed electrochemical aptasensor for ultra-sensitive detection of soluble PD-L1 in breast cancer based on decorated covalent organic frameworks and carbon nanotubes. *Anal. Chim. Acta* **2023**, *1282*, 341927.

(18) Wang, W.; Geng, L.; Zhang, Y.; Shen, W.; Bi, M.; Gong, T.; Hu, Z.; Guo, C.; Wang, T.; Sun, T. Development of antibody-aptamer sandwich-like immunosensor based on RCA and Nicked-PAM CRISPR/Cas12a system for the ultra-sensitive detection of a biomarker. *Anal. Chim. Acta* **2023**, *1283*, 341849.

(19) Zhen, D.; Zhang, S.; Yang, A.; Ma, Q.; Deng, Z.; Fang, J.; Cai, Q.; He, J. A supersensitive electrochemical sensor based on RCA amplification-assisted "silver chain"-linked gold interdigital electrodes and CRISPR/Cas9 for the detection of Staphylococcus aureus in food. *Food Chem.* **2024**, *440*, 138197.

(20) Zhang, Q.; Zhang, M.; Guo, Z.; Li, J.; Zhu, Z.; Wang, Y.; Liu, S.; Huang, J.; Yu, J. DNA tetrahedron-besieged primer and DNAzyme-activated programmatic RCA for low-background electrochemical detection of ochratoxin A. *Anal. Chim. Acta* **2023**, *1242*, 340782.

(21) Jiang, Y.; Qiu, Z.; Le, T.; Zou, S.; Cao, X. Developing a dual-RCA microfluidic platform for sensitive E. coli O157:H7 whole-cell detections. *Anal. Chim. Acta* **2020**, *1127*, 79−88.

(22) Wang, J.; Liu, J. N.; Thomsen, J.; Selnihhin, D.; Hede, M. S.; Kirsebom, F. C. M.; Franch, O.; Fjelstrup, S.; Stougaard, M.; Ho, Y. P.; Pedersen, F. S.; Knudsen, B. R. Novel DNA sensor system for highly sensitive and quantitative retrovirus detection using virus encoded integrase as a biomarker. *Nanoscale* **2017**, *9* (1), 440−448.

(23) Kong, H.; Zhang, W.; Yao, J.; Li, C.; Lu, R.; Guo, Z.; Li, J.; Li, C.; Li, Y.; Zhang, C.; Zhou, L. A RT-LAMP based hydrogen ion selective electrode sensing for effective detection HIV-1 RNA with high-sensitivity. *Sens. Actuators, B* **2021**, *329*, 129118.

(24) Ajbani, S. P.; Velhal, S. M.; Kadam, R. B.; Patel, V. V.; Bandivdekar, A. H. Immunogenicity of Semliki Forest virus based self-amplifying RNA expressing Indian HIV-1C genes in mice. *Int. J. Biol. Macromol.* **2015**, *81*, 794−802.

(25) McClure, P.; Curran, R.; Boneham, S.; Ball, J. K. A polymerase chain reaction method for the amplification of full-length envelope

https://doi.org/10.1021/acsomega.4c02229
ACS Omega 2024, 9, 25042−25053

genes of HIV-1 from DNA samples containing single molecules of HIV-1 provirus. *J. Virol. Methods* **2000**, *88* (1), 73−80.
(26) Guha, T. K.; Calos, M. P. Nucleofection of phiC31 Integrase Protein Mediates Sequence-Specific Genomic Integration in Human Cells. *J. Mol. Biol.* **2020**, *432* (13), 3950−3955.
(27) Jonsson, C. B.; Donzella, G. A.; Roth, M. J. Characterization of the forward and reverse integration reactions of the Moloney murine leukemia virus integrase protein purified from Escherichia coli. *J. Biol. Chem.* **1993**, *268* (2), 1462−1469.
(28) Medina-De la Garza, C. E.; Castro-Corona, M. d. l. A.; Salinas-Carmona, M. C. Near misdiagnosis of acute HIV-infection with ELISA-Western Blot scheme: Time for mindset change. *IDCases* **2021**, *25*, No. e01168.
(29) Cárdenas, A. M.; Baughan, E.; Hodinka, R. L. Evaluation of the Bio-Rad Multispot HIV-1/HIV-2 Rapid Test as an alternative to Western blot for confirmation of HIV infection. *J. Clin. Virol.* **2013**, *58*, e97−e103.
(30) Cajazeiras, J. B.; Melo, L. M.; Albuquerque, E. S.; Rdis-Baptista, G.; Cavada, B. S.; Freitas, V. J. F. Analysis of protein expression and a new prokaryotic expression system for goat (Capra hircus) spermadhesin Bdh-2 cDNA. *Genet. Mol. Res.* **2009**, *8* (3), 1147−1157.
(31) Sharma, S. Pharmacological mechanism of indigenous herb Exacum lawii on cisplatin instigated toxicity in human embryonic kidney cells (HEK-293). *Phytomedi. Plus* **2023**, *3* (2), 100454.
(32) Sohrab, S. S.; El-Kafrawy, S. A.; Azhar, E. I. Effect of insilico predicted and designed potential siRNAs on inhibition of SARS-CoV-2 in HEK-293 cells. *J. King Saud Univ., Sci.* **2022**, *34* (4), 101965.
(33) Bakhshizadeh Gashti, A.; Chahal, P. S.; Gaillet, B.; Garnier, A. Purification of recombinant vesicular stomatitis virus-based HIV vaccine candidate. *Vaccine* **2023**, *41* (13), 2198−2207.
(34) Grinsztejn, B.; Nguyen, B.-Y.; Katlama, C.; Gatell, J. M.; Lazzarin, A.; Vittecoq, D.; Gonzalez, C. J.; Chen, J.; Harvey, C. M.; Isaacs, R. D. Safety and efficacy of the HIV-1 integrase inhibitor raltegravir (MK-0518) in treatment-experienced patients with multi-drug-resistant virus: a phase II randomised controlled trial. *Lancet* **2007**, *369* (9569), 1261−1269.
(35) Moradbeigi, M.; SeyedAlinaghi, S.; Sajadipour, M.; Dadras, O.; Shojaei, E.; Ahmadi, P.; Bayanolhagh, S.; Baesi, K.; Rasoolinejad, M. The relationship between HIV antibody titer, HIV viral load, HIV p24 Antigen, and CD4 T-cell count among iranian HIV-positive patients. *Infect. Disord.: Drug Targets* **2020**, *20* (5), 752−757.
(36) Lin, H. J.; Haywood, M.; Hollinger, F. B. Application of a commercial kit for detection of PCR products to quantification of human immunodeficiency virus type 1 RNA and proviral DNA. *J. Clin. Microbiol.* **1996**, *34* (2), 329−333.
(37) Van Kerckhoven, I.; Fransen, K.; Peeters, M.; De Beenhouwer, H.; Piot, P.; van der Groen, G. Quantification of human immunodeficiency virus in plasma by RNA PCR, viral culture, and p24 antigen detection. *J. Clin. Microbiol.* **1994**, *32* (7), 1669−1673.

https://doi.org/10.1021/acsomega.4c02229
ACS Omega 2024, 9, 25042−25053